

cations, e.g. 395  $\text{cm}^{-1}$  for  $\text{CH}_3\text{CF}_3\text{SI}^+\text{AsF}_6^{-13}$  or 332  $\text{cm}^{-1}$  in  $(\text{CH}_3)_2\text{SI}^+\text{AsF}_6^{-12}$ . The Ra frequencies of  $\text{S}_7\text{X}^+\text{MF}_6^-$  confirm the results of the IR data (Table II) and are in good agreement with the Ra spectrum of solid  $\text{S}_7\text{O}$ .

**Acknowledgment.** We thank the Deutsche Forschungsgemeinschaft (DFG) and the Fonds der chemischen Industrie for financial support and Prof. Dr. T. N. Mitchell for his help in preparing the manuscript.

Contribution from the Department of Chemistry and Biochemistry, University of California, Los Angeles, California 90024-1569

## Synthesis and Structural Characterization of Metallocarborane Poly(pyrazolyl)borate Complexes

David M. Schubert, Carolyn B. Knobler, Swiatoslaw Trofimenko,<sup>1</sup> and M. Frederick Hawthorne\*

Received October 10, 1989

The mixed-ligand poly(1-pyrazolyl)borate-dicarbollide metallocarborane complexes *closo*-3- $(\eta^3\text{-HB}(\text{pz})_3)$ -3,1,2- $\text{RhC}_2\text{B}_9\text{H}_{11}$  (**3a**), *closo*-2- $(\eta^3\text{-HB}(\text{pz})_3)$ -2,1,7- $\text{RhC}_2\text{B}_9\text{H}_{11}$  (**3b**), and [*closo*-3- $(\eta^2\text{-Ph}_2\text{B}(\text{pz})_2)$ -3,1,2- $\text{NiC}_2\text{B}_9\text{H}_{11}$ ]<sup>-</sup> (**[5]<sup>-</sup>**) (pz = 1-pyrazolyl) have been prepared and characterized by a combination of spectroscopic techniques, elemental analysis, and X-ray crystallography. Complex **3a** crystallizes in the space group  $P2_1$  with  $a = 8.874$  (1) Å,  $b = 10.786$  (1) Å,  $c = 10.604$  (1) Å,  $\beta = 109.284$  (3)°,  $V = 960$  Å<sup>3</sup>, and  $Z = 2$ . Data were collected to a maximum of  $2\theta = 55^\circ$ , giving 2322 unique reflections. The final discrepancy index was  $R = 0.042$  ( $R_w = 0.054$ ) for 1969 independent reflections. Complex **3b** crystallizes in the space group  $C2/c$  with  $a = 14.830$  (2) Å,  $b = 27.059$  (3) Å,  $c = 20.298$  (2) Å,  $\beta = 108.907$  (3)°,  $V = 7706$  Å<sup>3</sup>, and  $Z = 16$ . Data were collected to a maximum of  $2\theta = 50^\circ$ , giving 4672 unique reflections. The final discrepancy index was  $R = 0.048$  ( $R_w = 0.063$ ) for 3525 independent reflections. Compound **[NMe<sub>4</sub>][5]** crystallizes in the space group  $P2_1/a$  with  $a = 17.437$  (6) Å,  $b = 9.631$  (3) Å,  $c = 19.695$  (4) Å,  $\beta = 92.271$  (8)°,  $V = 3305$  Å<sup>3</sup>, and  $Z = 4$ . Data were collected to a maximum of  $2\theta = 45^\circ$ , giving 4332 unique reflections. The final discrepancy index was  $R = 0.082$  ( $R_w = 0.091$ ) for 1585 independent reflections. The anion **[5]<sup>-</sup>** is oxidized by ferric chloride to the neutral species *closo*-3- $(\eta^2\text{-Ph}_2\text{B}(\text{pz})_2)$ -3,1,2- $\text{NiC}_2\text{B}_9\text{H}_{11}$  (**6**). NMR spectral data for **3a**, **3b**, and **[5]<sup>-</sup>** indicate fluxional solution behavior such that pyrazole ring environments are equilibrated on the NMR time scale. Complex **[5]<sup>-</sup>** exhibits an unusual carborane cage distortion resulting from an intramolecular influence of the axial phenyl group of the  $(\eta^2\text{-Ph}_2\text{B}(\text{pz})_2)^-$  ligand.

### Introduction

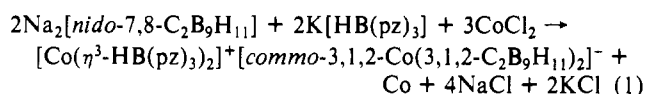
The poly(pyrazolyl)borate<sup>2</sup> and dicarbollide<sup>3</sup> ligands were perhaps the most significant new ligand types to be introduced in the 1960s; large subareas of coordination and organometallic chemistry have now developed around each of these ligand systems. Despite the extensive and parallel development of the transition-metal chemistry involving each of these ligand types, no examples of metal complexes containing both dicarbollide and poly(pyrazolyl)borate ligands bound to the same metal center have previously been reported. Herein we report the synthesis and structural characterization of the first mixed-ligand sandwich complexes that contain both of these boron-supported ligand systems.

Notably, both the tris(1-pyrazolyl)borate ( $[\text{RB}(\text{pz})_3]^-$ , pz = 1-pyrazolyl) and the isomeric dicarbollide ( $[\text{nido-C}_2\text{B}_9\text{H}_{11}]^{2-}$ ) ligands bear a relationship to the cyclopentadienide ( $[\text{C}_5\text{H}_5]^-$ ) ligand in so far as each of these ligands is capable of functioning as a six-electron donor in coordination compounds. Thus, either of these ligands may be used to form symmetrical bis(ligand) transition-metal complexes. However, these ligands differ from the cyclopentadienide ligand and from each other in important respects; the  $[\text{RB}(\text{pz})_3]^-$  ligands are uninegative  $\sigma$ -donors, whereas the  $[\text{nido-C}_2\text{B}_9\text{H}_{11}]^{2-}$  ligands are dinegative  $\pi$ -donors. The dicarbollide ligands are also capable of functioning as formal four-electron  $\pi$ -donors in the "slipped" bonding mode,<sup>3b</sup> and hence may be compared with the  $[\text{RB}(\text{pz})_3]^-$  ligands, which exhibit the  $\eta^2$ - $\sigma$ -bonding mode, as well as with the bidentate  $\sigma$ -donor bis(1-pyrazolyl)borate ( $[\text{R}_2\text{B}(\text{pz})_2]^-$ ) ligands.<sup>2</sup> The mixed-ligand sandwich complexes described herein represent the first examples

of formal 18-electron,  $d^6$  and  $d^8$  metal *closo*- $(\eta\text{-R}_n\text{B}(\text{pz})_{4-n})\text{M}$ - $(\text{C}_2\text{B}_9\text{H}_{11})$  ( $n = 1, 2$ ) species. Considering the great structural versatility of each of these ligand systems, innumerable other possibilities exist for mixed poly(pyrazolyl)borate-metallocarborane complexes.

### Results and Discussion

**Synthesis of Tris(1-pyrazolyl)borate Metallocarborane Complexes.** Initial attempts to prepare mixed poly(1-pyrazolyl)borate-dicarbollide transition-metal complexes by direct reactions of the ligands and metal salts were unsuccessful due to the formation of symmetrical bis(ligand) complexes. For example, attempts to directly prepare the unsymmetrical cobalt complex *closo*-3- $(\eta^3\text{-HB}(\text{pz})_3)$ -3,1,2- $\text{CoC}_2\text{B}_9\text{H}_{11}$  resulted in a high yield of an orange crystalline salt composed of the symmetrical cationic<sup>4</sup> and anionic<sup>3</sup> cobalt sandwich complexes, as shown in eq 1. This



salt was identified by a combination of NMR and IR spectroscopy and by a single-crystal X-ray analysis. This result was not unexpected since the formation of symmetrical bis(ligand) complexes is characteristic of the tris(1-pyrazolyl)borate ligand as a result of its excellent chelating ability.<sup>2</sup> Nevertheless, these results indicated that less direct methods were necessary to achieve the desired syntheses of unsymmetrical metal complexes containing both dicarbollide and poly(pyrazolyl)borate ligands.

The rhodacarborane complexes *closo*-3,3-( $\text{PPh}_3$ )<sub>2</sub>-3-Cl-3,1,2- $\text{RhC}_2\text{B}_9\text{H}_{11}$  (**1**) and *closo*-2-( $\text{PPh}_3$ )<sub>2</sub>-2-Cl-2,1,7- $\text{RhC}_2\text{B}_9\text{H}_{11}$  (**2**) are excellent precursors for species that contain the [3,1,2- $\text{RhC}_2\text{B}_9\text{H}_{11}$ ] and [2,1,7- $\text{RhC}_2\text{B}_9\text{H}_{11}$ ] metallocarborane moieties, respectively. These structurally characterized complexes are readily prepared derivatives of the corresponding rhodacarborane hydride species *closo*-3,3-( $\text{PPh}_3$ )<sub>2</sub>-3-H-3,1,2- $\text{RhC}_2\text{B}_9\text{H}_{11}$  and *closo*-2,2-

- (1) E. I. du Pont de Nemours & Co., Wilmington, DE.
- (2) (a) Trofimenko, S. *Acc. Chem. Res.* **1971**, *4*, 17. (b) Trofimenko, S. *Chem. Rev.* **1972**, *72*, 497. (c) Trofimenko, S. *Prog. Inorg. Chem.* **1986**, *34*, 115.
- (3) (a) Hawthorne, M. F.; Young, D. C.; Andrews, T. D.; Howe, D. V.; Pilling, R. L.; Pitts, A. D.; Reintjes, M.; Warren, L. F., Jr.; Wegner, P. A. *J. Am. Chem. Soc.* **1968**, *90*, 879. (b) Hawthorne, M. F. *Acc. Chem. Res.* **1968**, *1*, 281.

- (4) Trofimenko, S. *J. Am. Chem. Soc.* **1966**, *88*, 1842.

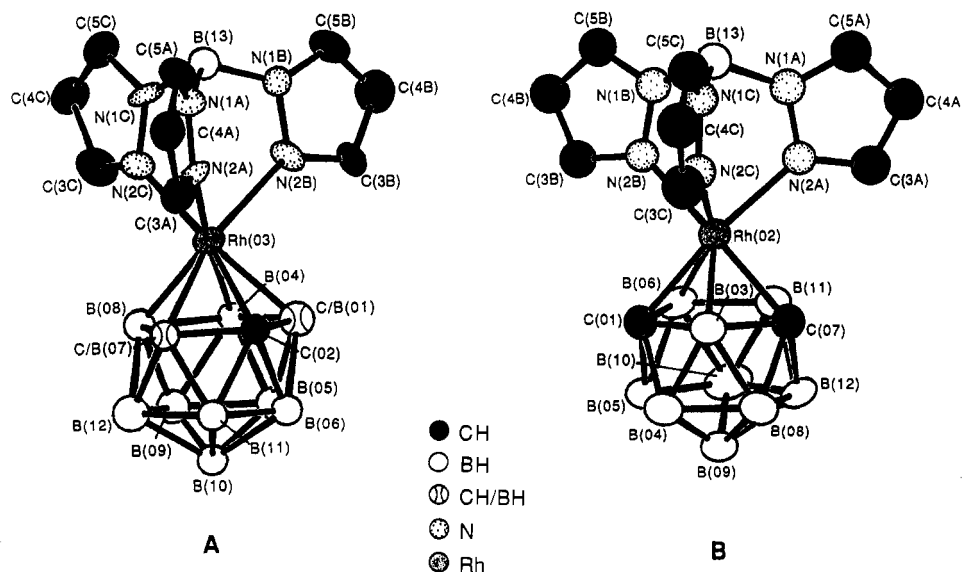
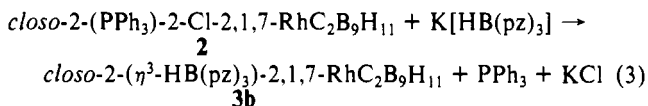
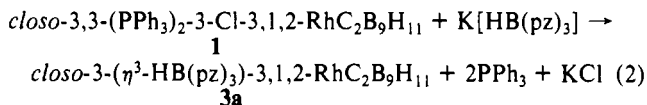


Figure 1. Structures (A) of *closo*-3-( $\eta^3$ -HB(pz)<sub>3</sub>)-3,1,2-RhC<sub>2</sub>B<sub>9</sub>H<sub>11</sub> (**3a**) and (B) *closo*-2-( $\eta^3$ -HB(pz)<sub>3</sub>)-2,1,7-RhC<sub>2</sub>B<sub>9</sub>H<sub>11</sub> (**3b**) with hydrogen atoms omitted for clarity.

(PPh<sub>3</sub>)<sub>2</sub>-2-H-2,1,7-RhC<sub>2</sub>B<sub>9</sub>H<sub>11</sub>.<sup>5</sup> The isomerism of the dicarbollide cages in **1** and **2** results in differences in the coordination number of rhodium, as well as in icosahedral cage distortions. Complex **2** can be regarded as a 16-electron rhodium complex, as indicated by the metal coordination number and overall *closo* cluster geometry, while **1** contains an 18-electron rhodium center. The use of these rhodacarborane reagents in the synthesis of mono(tris(1-pyrazolyl)borato)rhodium complexes parallels the synthetic method previously employed in the preparation of a number of rhodium (I) complexes containing the (HB(pz)<sub>3</sub>Rh) moiety.<sup>6</sup>

The reaction of complex **1** or **2** with K[HB(pz)<sub>3</sub>] (pz = 1-pyrazolyl) affords the corresponding mixed-ligand complexes, *closo*-3-( $\eta^3$ -HB(pz)<sub>3</sub>)-3,1,2-RhC<sub>2</sub>B<sub>9</sub>H<sub>11</sub> (**3a**) or *closo*-2-( $\eta^3$ -HB(pz)<sub>3</sub>)-2,1,7-RhC<sub>2</sub>B<sub>9</sub>H<sub>11</sub> (**3b**), respectively, in high yields, as illustrated by eqs 2 and 3. Complexes **3a** and **3b** were each isolated



as air-stable orange crystalline solids and were characterized by a combination of spectroscopic techniques, elemental analysis, and single-crystal X-ray diffraction studies.

The mass spectrum of each complex showed a strong parent ion envelope at  $m/e$  450 (calculated  $m/e$  450). The <sup>11</sup>B{<sup>1</sup>H} NMR spectra of **3a** and **3b** contained resonances in 2:1:3:1:2:1 and 2:1:2:1:1:2:1 area ratios, respectively, consistent with the local symmetry of each isomeric complex. The <sup>1</sup>H NMR spectrum of each complex displayed the expected resonances and intensities for [HB(pz)<sub>3</sub>]<sup>-</sup> ligands having three chemically equivalent pyrazole rings and for dicarbollide cages with equivalent carboranyl C-H groups. Proton resonances attributable to the B-H groups of each ligand could not be unambiguously assigned because of quadrupolar broadening by the isotopic boron nuclei. Pyrazole proton resonances occurred at chemical shift values that are comparable to those reported for other complexes that contain the [(HB(pz)<sub>3</sub>)Rh] moiety.<sup>6</sup>

Table I. Selected Interatomic Distances (Å) and Angles (deg) for 3- $\eta^3$ -HB(pz)<sub>3</sub>-3,1,2-RhC<sub>2</sub>B<sub>9</sub>H<sub>11</sub> (**3a**)

Distances			
Rh(03)-C(02)	2.134 (12)	Rh(03)-C/B(01)	2.164 (17)
Rh(03)-C/B(07)	2.127 (13)	Rh(03)-B(04)	2.197 (7)
Rh(03)-B(08)	2.19 (2)	Rh(03)-B(13)	3.230 (7)
Rh(03)-N(2A)	2.141 (5)	Rh(03)-N(2B)	2.14 (2)
Rh(03)-N(2C)	2.11 (2)	C(01)-C(02)	1.52 (2)
C(01)-B(04)	1.82 (2)	C(02)-B(07)	1.65 (2)
B(07)-B(08)	1.90 (2)	B(04)-B(08)	1.83 (2)
B(13)-N(1A)	1.534 (9)	B(13)-N(1B)	1.48 (3)
B(13)-N(1C)	1.57 (3)	N(1A)-N(5A)	1.358 (7)
N(1B)-N(5B)	1.43 (3)	N(1C)-N(5C)	1.33 (3)
Angles			
N(2A)-Rh(03)-N(2B)	84.6 (6)	Rh(03)-N(2A)-N(1A)	120.7 (9)
N(2B)-Rh(03)-N(2C)	80.4 (7)	Rh(03)-N(2B)-N(1B)	121.9 (13)
N(2A)-Rh(03)-N(2C)	88.0 (6)	Rh(03)-N(2C)-N(1C)	116.0 (15)
N(2A)-N(1A)-B(13)	118.4 (11)	N(1A)-B(13)-N(1B)	114.1 (11)
N(2B)-N(1B)-B(13)	115.0 (15)	N(1B)-B(13)-N(1C)	105.0 (13)
N(2C)-N(1C)-B(13)	125 (2)	N(1A)-B(13)-N(1C)	106.7 (11)

Stereochemical nonrigidity is commonly observed for poly(pyrazolyl)borate transition-metal complexes.<sup>2,6</sup> Sharp resonances in the <sup>1</sup>H NMR spectra of **3a** and **3b** attributable to three equivalent pyrazole rings are indicative of a similar dynamic process in solution, which averages the pyrazole proton environments on the NMR time scale. Previously reported studies indicate that fluxionality in poly(pyrazolyl)borate transition-metal complexes may be mediated by 16-electron complexes containing the  $\eta^2$ -HB(pz)<sub>3</sub> ligand rather than by axial rotation of ligands.<sup>2,6a,b</sup> In the present case, the rapid axial rotation of the dicarbollide cages of **3a** and **3b** in solution, which would also result in an averaging of the pyrazole ring environments, may also occur. This process is common for related 12-vertex rhodacarborane complexes.<sup>7</sup> However, the steric nature of the [HB(pz)<sub>3</sub>]<sup>-</sup> ligand, as discussed below, may inhibit this dynamic process.

**Description of the Molecular Structures of 3a and 3b.** The structures of the isomeric complexes **3a** and **3b** are shown in Figure 1. Tables I and II list selected interatomic distances and angles for complexes **3a** and **3b**, respectively. Complex **3a** exhibited crystallographic disorder resulting from the presence of two rotational conformers of the dicarbollide cage superimposed such that only one atom of the C<sub>2</sub>B<sub>2</sub> bonding face could be assigned as carbon. The two adjacent atoms were treated as half carbon, half boron. Disorder of this type is fairly common for metallacarborane dicarbollide complexes.<sup>8</sup> The unit cell of **3b** contained

(5) Baker, R. T.; Delaney, M. S.; King, R. E., III; Knobler, C. B.; Long, J. A.; Marder, T. B.; Paxson, T. E.; Teller, R. G.; Hawthorne, M. F. *J. Am. Chem. Soc.* **1984**, *106*, 2965.

(6) (a) Trofimenko, S. *J. Am. Chem. Soc.* **1969**, *91*, 588. (b) O'Sullivan, D. J.; Lalor, F. J. *J. Organomet. Chem.* **1974**, *65*, C47-C49. (c) King, R. B.; Bond, A. *J. Organomet. Chem.* **1974**, *73*, 115.

(7) Marder, T. B.; Baker, R. T.; Long, J. A.; Doi, J. A.; Hawthorne, M. F. *J. Am. Chem. Soc.* **1981**, *103*, 2988.

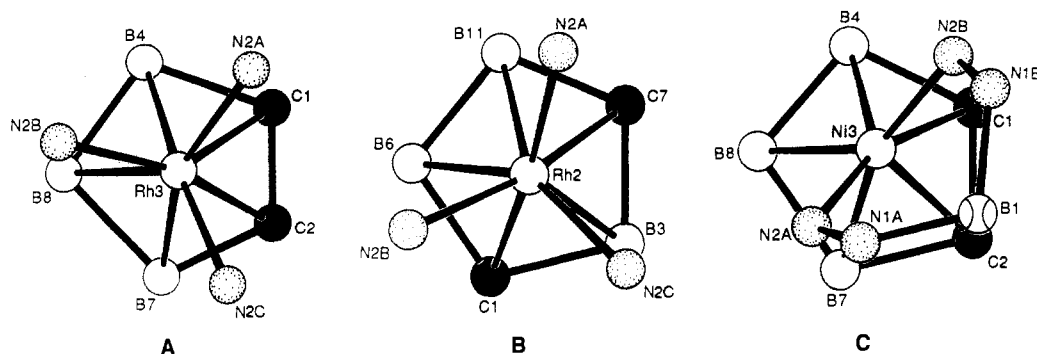


Figure 2. Projections of the  $\text{RhN}_3$  fragments of (A) **3a**, (B) **3b**, and (C) the  $\text{NiN}_4\text{B}$  fragment of **[5]**<sup>-</sup> onto the  $\text{C}_2\text{B}_3$  bonding faces.

two crystallographically unique molecules, designated **3b** and **3b'**. These molecules were found to be nearly identical in a structural sense, differing only slightly in the rotational conformation of the  $[(\text{HB}(\text{pz})_3)\text{Rh}]$  moiety with respect to the dicarbollide cage and in small differences in the 12-vertex  $\text{RhC}_2\text{B}_9\text{H}_{11}$  cage geometry, as discussed below. Hence, these two crystallographic forms will be treated here as one complex. Interatomic distances and angles, as well as positional and thermal parameters are tabulated separately for each independent molecule in Table II. The isomeric **3a** and **3b** complexes contain nearly identical rigid  $[(\eta^3\text{-HB}(\text{pz})_3)\text{Rh}]$  fragments of local (noncrystallographic)  $\text{C}_{3v}$  symmetry.

Distortions from idealized closo geometry for metallacarborane dicarbollide complexes have been a subject of considerable interest. Previous comparisons between isomeric  $\text{d}^8\text{-}3,1,2\text{-RhC}_2\text{B}_9\text{H}_{11}$  and  $\text{d}^8\text{-}2,1,7\text{-RhC}_2\text{B}_9\text{H}_{11}$  rhodacarboranes have shown rather dramatic structural differences.<sup>9</sup> The crystal structures of **3a** and **3b** provide an opportunity to make similar comparisons for isomeric  $\text{d}^6$ -rhodacarborane complexes containing identical metal vertices. However, as predicted for  $\text{d}^6$ -metal complexes, **3a** and **3b** exhibit very little distortion from idealized closo geometry and thus show only small distortional differences from one another.

In the case of **3a**, the slipping parameter  $\Delta$ <sup>10</sup> is negligibly small (0.01 Å). The determination of folding parameters<sup>11</sup> for this complex is complicated somewhat by the crystallographic disorder; however, this species can be seen to contain a nearly planar  $\text{C}_2\text{B}_3$  face with angles between the two possible sets of  $\text{B-C-C-B}$  and  $\text{B-B-B}$  planes of less than  $2^\circ$ . The two crystallographically unique molecules **3b** and **3b'** are also virtually unslipped. The bonding face in each of these complexes shows a small distortion from planarity such that the two carbon atoms are bent somewhat into the cage and toward the lower  $\text{B}_5$  belt. The resultant angle between the  $\text{C}(1)\text{-B}(6)\text{-B}(11)\text{-C}(7)$  and  $\text{C}(1)\text{-B}(3)\text{-C}(7)$  planes is  $6.9^\circ$  for **3b**. Although slight for this  $\text{d}^6$  complex, it is notable that this type of folding distortion occurs to a much greater degree in the related  $\text{d}^8$ -rhodacarborane anion  $[\text{closo-}2,2\text{-}(\text{PPh}_3)_2\text{-}2,1,7\text{-RhC}_2\text{B}_9\text{H}_{11}]^-$ ,<sup>9</sup> as well as in a number of other  $2,1,7\text{-MC}_2\text{B}_9\text{H}_{11}$  complexes.<sup>12</sup> The dicarbollide cage in **3b'** may possess some degree of crystallographic disorder, as indicated by its anomalous interatomic distances at the bonding face. This disorder may be caused by the presence of a superimposed minor occupant that contains a mirror image dicarbollide cage in which atom positions

Table II. Selected Interatomic Distances (Å) and Angles (deg) for the Two Crystallographic Forms of  $2\text{-}(\eta^3\text{-HB}(\text{pz})_3)\text{-}2,1,7\text{-RhC}_2\text{B}_9\text{H}_{11}$  (**3b/3b'**)

Distances for <b>3b</b>			
Rh(02)-C(01)	2.169 (7)	Rh(02)-C(07)	2.165 (7)
Rh(02)-B(03)	2.146 (9)	Rh(02)-B(06)	2.156 (10)
Rh(02)-B(11)	2.162 (9)	Rh(02)-N(2A)	2.099 (5)
Rh(02)-N(2B)	2.103 (5)	Rh(02)-N(2C)	2.219 (7)
Rh(02)-B(13)	3.241 (8)	C(01)-B(03)	1.737 (12)
B(03)-C(07)	1.713 (13)	C(07)-B(11)	1.719 (14)
B(06)-B(11)	1.788 (12)	C(01)-B(06)	1.729 (14)
B(13)-N(1A)	1.517 (10)	B(13)-N(1B)	1.530 (10)
B(13)-N(1C)	1.521 (12)	N(1A)-N(2A)	1.367 (7)
N(1B)-N(2B)	1.363 (7)	N(1C)-N(2C)	1.380 (8)
Angles for <b>3b</b>			
N(2A)-Rh(02)-N(2B)	88.5 (2)	Rh(02)-N(2A)-N(1A)	120.5 (4)
N(2A)-N(1A)-B(13)	120.4 (6)	N(1A)-B(13)-N(1B)	109.6 (6)
N(2A)-Rh(02)-N(2C)	82.9 (2)	Rh(02)-N(2B)-N(1B)	119.8 (4)
N(2B)-N(1B)-B(13)	120.8 (6)	N(1A)-B(13)-N(1C)	108.6 (6)
N(2B)-Rh(02)-N(2C)	81.0 (2)	Rh(02)-N(2C)-N(1C)	117.8 (4)
N(2C)-N(1C)-B(13)	120.0 (6)	N(1B)-B(13)-N(1C)	106.4 (6)
Distances for <b>3b'</b>			
Rh(02')-C(01')	2.139 (10)	Rh(02')-B(03')	2.149 (11)
Rh(02')-B(06')	2.127 (11)	Rh(02')-C(07')	2.179 (8)
Rh(02')-B(11')	2.163 (9)	Rh(02')-N(2A')	2.136 (6)
Rh(02')-N(2B')	2.111 (6)	Rh(02')-N(2C')	2.196 (6)
Rh(02')-B(13')	3.254 (10)	C(01')-B(03')	1.65 (2)
C(01')-B(06')	1.719 (15)	B(03')-C(07')	1.736 (16)
B(06')-B(11')	1.672 (15)	C(07')-B(11')	1.736 (14)
N(1A')-N(2A')	1.368 (9)	N(1B')-N(2B')	1.365 (9)
N(1C')-N(2C')	1.363 (9)	B(13')-N(1A')	1.538 (11)
B(13')-N(1B')	1.495 (14)	B(13')-N(1C')	1.542 (11)
Angles for <b>3b'</b>			
N(2A')-Rh(02')-N(2B')	86.7 (2)	N(1A')-B(13')-N(1B')	108.2 (7)
N(2A')-Rh(02')-N(2C')	81.9 (2)	N(1A')-B(13')-N(1C')	107.6 (7)
N(2B')-Rh(02')-N(2C')	82.8 (2)	N(1B')-B(13')-N(1C')	108.2 (7)
N(2A')-N(1A')-B(13')	120.5 (6)	Rh(02')-N(2A')-N(1A')	119.5 (4)
N(2B')-N(1B')-B(13')	121.0 (6)	Rh(02')-N(2B')-N(1B')	120.6 (4)
N(2C')-N(1C')-B(13')	120.2 (6)	Rh(02')-N(2C')-N(1C')	118.9 (4)

are interchanged across the mirror plane passing through  $\text{B}(11)$  and through the midpoint between  $\text{C}(1)$  and  $\text{B}(3)$ . The apparent disorder results in an artificial decrease of the folding distortion for this complex.

Projections of the  $\text{MN}_3$  fragments of **3a** and **3b** onto the  $\text{C}_2\text{B}_3$  bonding face of each complex are shown in Figure 2. In each of these complexes the superposition of the local  $\text{C}_{3v}$  symmetry  $[(\text{HB}(\text{pz})_3)\text{Rh}]$  fragment onto the five-membered face of the dicarbollide requires that one pyrazole ring approaches an eclipsed conformation with an atom in the cage bonding face. In addition, the terminal  $\text{B-H}$  and  $\text{C-H}$  groups of the  $\text{C}_2\text{B}_3$  belt of the dicarbollide ligand tilt above the plane of the cage bonding face ( $\text{H}$  in the direction away from the cage) with an elevation angle of approximately  $22^\circ$ . This results in at least one relatively close contact between a hydrogen atom at a pyrazole  $\text{C}(3)$  position and a carborane cage hydrogen atom in **3a** and **3b**. These steric interactions may destabilize the  $\eta^3$ -bonding mode when in a fully eclipsed conformation and may require the observed fluxionality to be mediated via 16-electron rhodium intermediates involving the  $\eta^2\text{-HB}(\text{pz})_3$  ligand rather than by axial cage rotation. Attempts to prepare analogous complexes bearing the  $[\text{HB}(3\text{-Phpz})_3]^-$  and  $[\text{HB}(3,5\text{-Me}_2\text{pz})_3]^-$  ligands have as yet been unsuccessful, possibly owing to the steric congestion near the 3-carbon region.

- (8) For example, see: Hardy, G. E.; Callahan, K. P.; Strouse, C. E.; Hawthorne, M. F. *Acta Crystallogr., Sect. B* **1976**, *B32*, 264.  
 (9) Walker, J. A.; Knobler, C. B.; Hawthorne, M. F. *Inorg. Chem.* **1985**, *24*, 2688.  
 (10) The slip parameter,  $\Delta$ , is defined as the displacement of the metal atom normal to the centroid of the least-squares plane of the lower  $\text{B}_5$  ring of the dicarbollide cage.  
 (11) The folding parameters,  $\theta$  and  $\phi$ , which measure the lack of coplanarity of the  $\text{C}_2\text{B}_3$  metal-bonding face with respect to the lower  $\text{B}_5$  plane, are the dihedral angles between the normal to the least-squares plane of the lower  $\text{B}_5$  ring and the  $\text{B}(4)\text{-C}(1)\text{-C}(2)\text{-B}(7)$  and  $\text{B}(4)\text{-B}(8)\text{-B}(7)$  planes, respectively, for  $3,1,2\text{-MC}_2\text{B}_9$  complexes, and the  $\text{C}(1)\text{-B}(6)\text{-B}(11)\text{-C}(7)$  and  $\text{C}(1)\text{-B}(3)\text{-C}(7)$  planes, respectively, for  $2,1,7\text{-MC}_2\text{B}_9$  complexes.  
 (12) (a) Miller, S. B.; Hawthorne, M. F. *J. Chem. Soc., Chem. Commun.* **1976**, 786. (b) King, R. E., III; Miller, S. B.; Knobler, C. B.; Hawthorne, M. F. *Inorg. Chem.* **1983**, *22*, 3548.

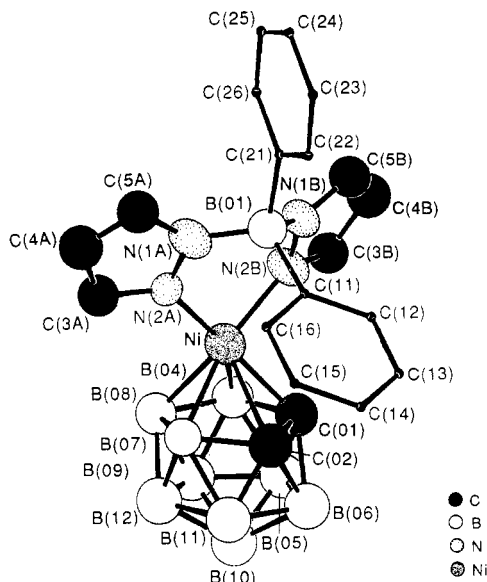
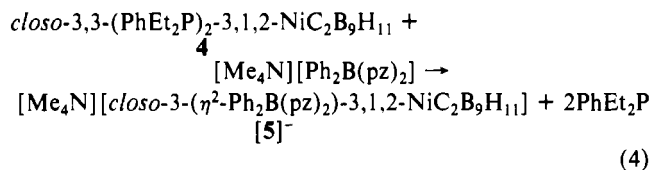


Figure 3. Structure of [*closo*-3-( $\eta^2$ -Ph<sub>2</sub>B(pz)<sub>2</sub>)-3,1,2-NiC<sub>2</sub>B<sub>9</sub>H<sub>11</sub>]<sup>-</sup> ([5]<sup>-</sup>) with hydrogen atoms omitted for clarity.

**Synthesis of a Bis(1-pyrazolyl)borate Metallacarborane Complex.** An extensive series of bis(phosphine) nickelacarborane complexes of the type *closo*-3,3-(R<sub>3</sub>P)<sub>2</sub>-3,1,2-NiC<sub>2</sub>B<sub>9</sub>H<sub>11</sub> (R = aryl, alkyl, or combinations thereof) have previously been prepared and characterized.<sup>12</sup> These complexes, which are easily prepared and handled, serve as excellent synthetic reagents in ligand displacement reactions. The reaction of 3,3-(PhMe<sub>2</sub>P)<sub>2</sub>-3,1,2-NiC<sub>2</sub>B<sub>9</sub>H<sub>11</sub> (**4**)<sup>13</sup> with [Me<sub>4</sub>N][Ph<sub>2</sub>B(pz)<sub>2</sub>] (pz = 1-pyrazolyl) in tetrahydrofuran affords the anionic mixed-ligand complex [*closo*-3-( $\eta^2$ -Ph<sub>2</sub>B(pz)<sub>2</sub>)-3,1,2-NiC<sub>2</sub>B<sub>9</sub>H<sub>11</sub>]<sup>-</sup> ([5]<sup>-</sup>) in good yield, as illustrated by eq 4.



The tetramethylammonium salt of [5]<sup>-</sup> was isolated as an air-stable pale red crystalline solid. This salt was characterized by a combination of spectroscopic techniques, elemental analysis, and a single-crystal X-ray diffraction study. The <sup>11</sup>B{<sup>1</sup>H} NMR spectrum of [5]<sup>-</sup> in acetone solution revealed a 1:1:2:1:2:2:1 pattern consistent with the local symmetry of the dicarbollide ligand. The <sup>1</sup>H NMR spectrum of this salt contained a single carborene C-H resonance, a set of resonances corresponding to two equivalent pyrazole rings, and a single broad resonance attributable to two equivalent phenyl groups. These spectral data are indicative of dynamic solution behavior that interconverts the axial and equatorial phenyl groups. Such stereochemical nonrigidity is commonly observed for [Ph<sub>2</sub>B(pz)<sub>2</sub>]<sup>-</sup> complexes.<sup>2</sup> For example, the complex (Me<sub>2</sub>B(pz)<sub>2</sub>)<sub>2</sub>Ni has been shown to undergo rapid interconversion of axial and equatorial methyl groups.<sup>14</sup>

**Description of the Molecular Structure of [Me<sub>4</sub>N][5].** The structure of the [5]<sup>-</sup> anion is shown in Figure 3. Selected interatomic distances and angles are given in Table III. The six-membered Ni(N<sub>2</sub>)<sub>2</sub>B ring of this anion exhibits the boat conformation characteristic of M( $\eta^2$ -Ph<sub>2</sub>B(pz)<sub>2</sub>) complexes.<sup>2</sup> The dihedral angles between the N<sub>4</sub> plane and the NiN<sub>2</sub> and BN<sub>2</sub> planes are 153.6 and 134.6°, respectively. This conformation results in an out-of-plane bending of the pyrazole rings, the dihedral angle between these rings being 36.0°. The Ni-B<sub>pz</sub> distance

Table III. Selected Interatomic Distances (Å) and Angles (deg) for [3-( $\eta^2$ -Ph<sub>2</sub>B(pz)<sub>2</sub>)-3,1,2-NiC<sub>2</sub>B<sub>9</sub>H<sub>11</sub>]<sup>-</sup> ([5]<sup>-</sup>)

Distances			
Ni(3)-C(01)	2.045 (14)	Ni(3)-C(02)	2.262 (15)
Ni(3)-B(04)	2.10 (2)	Ni(3)-B(07)	2.09 (2)
Ni(3)-B(08)	2.15 (2)	Ni(3)-N(2A)	1.914 (9)
Ni(03)-N(2B)	1.943 (12)	B(01)-N(1A)	1.52 (2)
B(01)-N(1B)	1.60 (2)	N(1A)-N(2A)	1.352 (15)
N(1B)-N(2B)	1.359 (16)	C(01)-C(02)	1.62 (2)
C(02)-B(07)	1.70 (2)	B(04)-B(08)	1.74 (2)
B(07)-B(08)	1.80 (2)	B(01)-C(11)	1.61 (2)
B(01)-C(21)	1.68 (2)		

Angles			
N(2A)-Ni(3)-N(2B)	91.9 (5)	B(01)-N(1A)-N(2A)	120.7 (11)
Ni(3)-N(2A)-N(1A)	123.3 (8)	C(11)-B(01)-C(21)	113.4 (11)
N(1A)-B(01)-N(1B)	107.0 (12)	B(01)-N(1B)-N(2B)	118.3 (11)
Ni(3)-N(2B)-N(1B)	123.6 (9)		

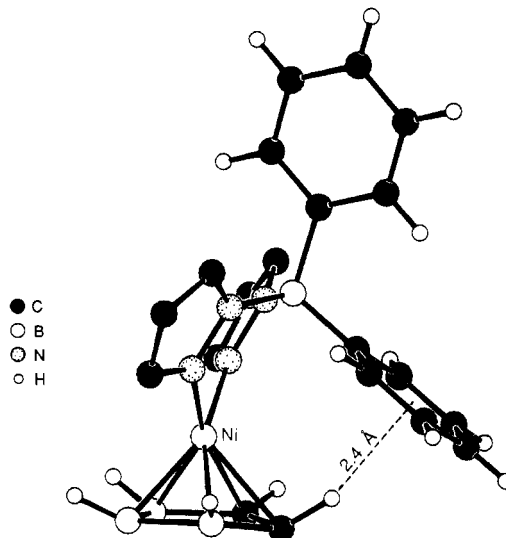


Figure 4. View of the [5]<sup>-</sup> anion with all boron atoms omitted except those of the C<sub>2</sub>B<sub>3</sub> bonding face and all pyrazole ring hydrogen atoms omitted for clarity.

is 3.20 Å. The phenyl groups are oriented with a dihedral angle of 78.9°. The distance between the ortho-hydrogen of the equatorial phenyl group and the centroid of the axial phenyl group is 3.1 Å. The apparent fluxionality of [5]<sup>-</sup> presumably involves inversion of the NiN<sub>4</sub>B boat conformation.

A projection of the NiN<sub>4</sub>B ring onto the C<sub>2</sub>B<sub>3</sub> dicarbollide cage face is shown in Figure 2. The plane of the NiN<sub>2</sub> fragment lies nearly perpendicular (89.8°) to the least-squares plane of the C<sub>2</sub>B<sub>3</sub> bonding face. The plane of the NiN<sub>2</sub> fragment is rotated with respect to the noncrystallographic local mirror plane of the dicarbollide cage, which passes through unique boron B(8) and the midpoint between C(1) and C(2) by a dihedral angle of 56°. This orientation places the NiN<sub>2</sub> plane parallel to the planes passing through C(1), B(7) and B(4), B(8) of the cage face. This rotational conformation is in conflict with the most stable conformation of d<sup>8</sup>-L<sub>2</sub>M<sup>2+</sup> dicarbollide complexes predicted by theory, in which the ML<sub>2</sub> fragment is oriented perpendicular to the local mirror plane of the C<sub>2</sub>B<sub>9</sub>H<sub>11</sub> cage.<sup>15</sup>

Metallacarborane dicarbollide complexes bearing d<sup>8</sup>-metal centers frequently exhibit marked distortions from idealized *closo* geometry, although considerable variation has been noted for members of this class. For example, the 3,1,2-MC<sub>2</sub>B<sub>9</sub>H<sub>11</sub> containing the  $\eta^2$ -[C<sub>2</sub>H<sub>4</sub>(NMe<sub>2</sub>)<sub>2</sub>Pd,<sup>16</sup> (Et<sub>3</sub>P)<sub>2</sub>Pt,<sup>15a</sup> and (Me<sub>3</sub>P)<sub>2</sub>Pd<sup>16</sup> vertices show large ( $\Delta = 0.52, 0.47$  Å) and moderate ( $\Delta = 0.26$  Å) slip distortions, respectively. The d<sup>8</sup>-rhodacarborane anion [3,3-(PPH<sub>3</sub>)<sub>2</sub>-3,1,2-RhC<sub>2</sub>B<sub>9</sub>H<sub>11</sub>]<sup>-</sup>, on the other hand, is essentially

(13) Schubert, D. M.; Knobler, C. B.; Hawthorne, M. F. Submitted for publication.

(14) Herring, F. G.; Patmore, D. J.; Storr, A. *J. Chem. Soc., Dalton Trans.* **1975**, 711.

(15) (a) Mingos, D. M. P.; Forsyth, M. I.; Welch, A. *J. Chem. Soc., Dalton Trans.* **1978**, 1363. (b) Mingos, D. M. P. *J. Chem. Soc., Dalton Trans.* **1977**, 602.

(16) Colquhoun, H. M.; Greenhough, T. J.; Wallbridge, M. G. H. *J. Chem. Soc., Chem. Commun.* **1978**, 322.

Table IV. Details of Crystallographic Collections<sup>a</sup>

	3a <sup>b</sup>	3b <sup>c</sup>	[NMe <sub>4</sub> ][5]
cryst size/mm	0.07 × 0.19 × 0.43	0.25 × 0.25 × 0.25	0.15 × 0.08 × 0.41
appearance	orange needle	orange parallelepiped	brown-red needle
space group	<i>P</i> 2 <sub>1</sub>	<i>C</i> 2/ <i>c</i>	<i>P</i> 2 <sub>1</sub> / <i>a</i>
<i>a</i> /Å	8.874 (1)	14.830 (2)	17.437 (6)
<i>b</i> /Å	10.786 (1)	27.059 (3)	9.631 (3)
<i>c</i> /Å	10.604 (1)	20.298 (2)	19.695 (4)
β/deg	109.284 (3)	108.907 (3)	92.271 (8)
<i>V</i> /Å <sup>3</sup>	960	7706	3305
<i>Z</i>	2	16	4
ρ(calcd)/g cm <sup>-3</sup>	1.55	1.54	1.1
μ/cm <sup>-1</sup>	8.1 (na)	8.02 (na)	6.6 (na)
scan width			
below Kα <sub>1</sub>	1.3	1.3	1.3
above Kα <sub>2</sub>	1.6	1.6	1.6
scan rate/deg min <sup>-1</sup>	4.5	9.0	6.0
no. of unique reflcns	2322	4672	4332
no. of obsd ( <i>I</i> > 3σ( <i>I</i> )) rflcns	1969	3525	1585
2θ max/deg	55	50	45
data collcd	+ <i>h</i> , + <i>k</i> , ± <i>l</i>	+ <i>h</i> , + <i>k</i> , ± <i>l</i>	<i>h</i> , <i>k</i> , ± <i>l</i>
no. of params refined	192	345	190
<i>R</i>	0.042	0.048	0.082
<i>R</i> <sub>w</sub>	0.054	0.063	0.091
GOF	1.72	2.06	1.93

<sup>a</sup> Conditions: *T* = 298 K; radiation (graphite monochromator), Mo Kα; wavelength, 0.7107 Å. <sup>b</sup> C<sub>11</sub>H<sub>21</sub>N<sub>6</sub>B<sub>10</sub>Rh. <sup>c</sup> C<sub>11</sub>H<sub>21</sub>N<sub>6</sub>B<sub>10</sub>Rh. <sup>d</sup> C<sub>20</sub>H<sub>27</sub>N<sub>4</sub>B<sub>10</sub>Ni.

unslipped ( $\Delta = 0.05 \text{ \AA}$ ).<sup>10</sup> These differences have been rationalized in terms of ligand effects on metal electron densities coupled with metal p-d promotion energies. Anion [5]<sup>-</sup>, like its bis(phosphine) analogue, 4,<sup>13</sup> shows no distortions from idealized *closo* geometry in the usual sense as measured by the distortion parameters referred to above. This is in keeping with the smaller p-d promotion energy of nickel as compared with palladium and platinum. However, the solid-state structure of [5]<sup>-</sup> does exhibit an unusual distortion that is imposed by the  $[\eta^2\text{-Ph}_2\text{B}(\text{pz})_2]^-$  ligand. The rotational and boat conformations of the Ni( $\eta^2\text{-Ph}_2\text{B}(\text{pz})_2$ ) moiety bring the axial phenyl group of the  $[\text{Ph}_2\text{B}(\text{pz})_2]^-$  ligand into close proximity to the hydrogen atom at the C(2) atom of the C<sub>2</sub>B<sub>3</sub> cage face, as illustrated in Figure 4. This interaction produces a distortion in the carborane cage in which the C(2) atom is bent down out of the plane of the five-membered bonding face toward the lower B<sub>3</sub> belt of the dicarbollide cage. The resultant dihedral angle between the C(1)–B(4)–B(7)–B(8) and C(1)–C(2)–B(7) planes is 9.2°. As a consequence, the Ni–C(2) interatomic distance is lengthened to 2.26 Å as compared with the Ni–C(1) distance of 2.04 Å. The nickel atom is not slipped with respect to the C<sub>2</sub>B<sub>3</sub> cage face and lies nearly equidistant from the atoms C(1), B(4), B(7), and B(8) with an average interatomic distance of 2.09 Å. The distance between H(2) and the plane of the axial phenyl group is 2.4 Å (2.5 Å from the phenyl ring centroid).

Oxidation of [Me<sub>4</sub>N][5] with anhydrous ferric chloride in ethanol resulted in a deep red paramagnetic complex, which has been identified as the neutral d<sup>7</sup> nickelacarborane, *closo*-3-( $\eta^2\text{-Ph}_2\text{B}(\text{pz})_2$ )-3,1,2-NiC<sub>2</sub>B<sub>9</sub>H<sub>11</sub> (6). A preliminary X-ray diffraction study has shown this species to be virtually isostructural with [5]<sup>-</sup>.

## Experimental Section

**General Procedures and Materials.** All reactions were carried out under an atmosphere of dry and deoxygenated argon. Filtrations and other reaction workup procedures were performed in air. Methylene chloride and tetrahydrofuran were distilled from phosphorus pentoxide and sodium benzophenone ketyl, respectively, immediately before use. Other solvents were reagent grade and were used without further purification. K[HB(pz)<sub>3</sub>], K[Ph<sub>2</sub>B(pz)<sub>2</sub>], and Ti[*closo*-3,1,2-TiC<sub>2</sub>B<sub>9</sub>H<sub>11</sub>] were prepared using published procedures.<sup>2</sup> The metallocarborane reagents *closo*-3,3-(PPh<sub>3</sub>)<sub>2</sub>-3-Cl-3,1,2-RhC<sub>2</sub>B<sub>9</sub>H<sub>11</sub> (1) and *closo*-3-(PPh<sub>3</sub>)-3-Cl-2,1,7-RhC<sub>2</sub>B<sub>9</sub>H<sub>11</sub> (2) were prepared as described previously.<sup>5</sup> The nickelacarborane complex *closo*-3,3-(PhEt<sub>2</sub>P)<sub>2</sub>-3,1,2-NiC<sub>2</sub>B<sub>9</sub>H<sub>11</sub> (4) was prepared by using the general method reported previously for the synthesis of (PR<sub>3</sub>)<sub>2</sub>Ni(C<sub>2</sub>B<sub>9</sub>H<sub>11</sub>) compounds.<sup>12</sup>

**Physical Measurements.** The 200.1 and 500.1-MHz <sup>1</sup>H NMR spectra were obtained on Bruker WP-200 and AM-500 spectrometers, respectively. The 160.5-MHz <sup>11</sup>B spectra were obtained on the Bruker AM-500

instrument. The <sup>1</sup>H NMR spectra were referenced relative to residual protons in deuterated solvents. The <sup>11</sup>B NMR spectra were referenced relative to external BF<sub>3</sub>·OEt<sub>2</sub> with positive chemical shifts referring to lower field strength. Infrared spectra were recorded on a Beckman FT-1100 instrument. UV-visible spectra were obtained on a Hewlett Packard 8450A diode-array spectrophotometer. Mass spectra were obtained on an AEI, Limited, Model MS-902 sector-filled, double-focusing spectrometer. Elemental analyses were performed by Galbraith Laboratories, Inc., Knoxville, TN.

***closo*-3-( $\eta^2\text{-HB}(\text{pz})_3$ )-3,1,2-RhC<sub>2</sub>B<sub>9</sub>H<sub>11</sub> (3a).** A mixture of 250 mg (0.99 mmol) of K[HB(pz)<sub>3</sub>] (pz = 1-C<sub>3</sub>H<sub>3</sub>N<sub>2</sub>) and 753 mg (0.99 mmol) of *closo*-3-Cl-3,3-(PPh<sub>3</sub>)<sub>2</sub>-3,1,2-RhC<sub>2</sub>B<sub>9</sub>H<sub>11</sub> was refluxed in THF for 4 h. The resulting orange solution was filtered through Celite to remove precipitated KCl, and solvent was removed by rotary evaporation. Crude product was taken up in chloroform, the mixture was filtered through a fine frit, and the product was recrystallized by layering with absolute ethanol. A second recrystallization from chloroform/ethanol resulted in 361 mg (81% yield) of analytically pure orange needles of 3a (dec 286 °C). Spectral data: <sup>1</sup>H NMR (CDCl<sub>3</sub>, ambient temperature) δ 4.29 (s, area 2, carborane C–H), 6.28 (t, area 3), 7.70 (d, area 3), 8.13 ppm (d, area 3), <sup>11</sup>B[<sup>1</sup>H] NMR (CDCl<sub>3</sub>, ambient temperature) δ -18.9 (area 2), -18.3 (area 1), -4.9 (area 3), 1.9 (area 1) 3.1 (area 2), 10.3 ppm (area 1); characteristic IR (cm<sup>-1</sup>) 3137 (m), 3127 (m), 3044 (m), 2607 (s, B–H str), 2597 (s, B–H str), 2579 (s, B–H str), 2566 (s, B–H str), 2533 (s, B–H str), 2502 (s, B–H str), 1314 (s), 1237 (m), 1134 (m), 1116 (m), 1052 (s), 993 (m), 777 (s), 753 (s), 720 (m); mass spectrum, parent ion at *m/e* 450, [<sup>12</sup>C<sub>11</sub>H<sub>21</sub><sup>11</sup>B<sub>10</sub><sup>14</sup>N<sub>6</sub>Rh<sub>2</sub>]<sup>+</sup>; UV-vis λ<sub>max</sub> 228 nm. Anal. Calcd: C, 29.47; H, 4.72; N, 18.75; B, 24.11; Rh, 22.95. Found: C, 29.35; H, 4.86; N, 18.32; B, 24.64; Rh, 21.74.

***closo*-2-( $\eta^2\text{-HB}(\text{pz})_3$ )-2,1,7-RhC<sub>2</sub>B<sub>9</sub>H<sub>11</sub> (3b).** The same procedure was followed as for the synthesis of 3a by using 250 mg (0.99 mmol) of K[HB(pz)<sub>3</sub>] (pz = 1-C<sub>3</sub>H<sub>3</sub>N<sub>2</sub>) and 528 mg (0.99 mmol) of *closo*-2-Cl-2-PPh<sub>3</sub>-2,1,7-RhC<sub>2</sub>B<sub>9</sub>H<sub>11</sub>. Analytically pure orange crystals of 3b (370 mg, 83% yield) were obtained by recrystallization from methylene chloride/*n*-pentane. Microcrystalline samples of 3b (dec 280 °C). Spectral data: <sup>1</sup>H NMR (CDCl<sub>3</sub>, ambient temperature) δ 2.78 (s, area 2, carborane C–H), 6.26 (t, area 3, pz C–H), 7.71 (d, area 3, pz C–H), 8.14 ppm (d, area 3, pz C–H); <sup>11</sup>B[<sup>1</sup>H] NMR (CDCl<sub>3</sub>, ambient temperature) δ -17.8 (area 2), -15.4 (area 1), -7.4 (area 2), -4.7 (area 1), 2.8 (area 1), 5.1 (area 2), 9.3 ppm (area 1); characteristic IR (cm<sup>-1</sup>) 3124 (w), 2584 (vs, B–H str), 2556 (s, B–H str), 1512 (w), 1499 (w), 1309 (m), 1221 (m), 1126 (m), 1049 (m), 792 (w), 761 (s), 717 (m); mass spectrum, parent ion at *m/e* 450, [<sup>12</sup>C<sub>11</sub>H<sub>21</sub><sup>11</sup>B<sub>10</sub><sup>14</sup>N<sub>6</sub>Rh<sub>2</sub>]<sup>+</sup>. Anal. Calcd: C, 29.47; H, 4.72; N, 18.75; B, 24.11; Rh, 22.95. Found: C, 29.26; H, 4.64; B, 18.45; N, 24.52; Rh, 21.83.

**[Me<sub>4</sub>N][*closo*-3-( $\eta^2\text{-Ph}_2\text{B}(\text{pz})_2$ )-3,1,2-NiC<sub>2</sub>B<sub>9</sub>H<sub>11</sub>] ([Me<sub>4</sub>N][5]).** A mixture of 541 mg (1.0 mmol) of Ti[*closo*-3,1,2-TiC<sub>2</sub>B<sub>9</sub>H<sub>11</sub>] and 462 mg (1.0 mmol) of (PhEt<sub>2</sub>P)<sub>2</sub>NiCl<sub>2</sub> in 150 mL of THF was stirred for 3 h. The resulting green solution was Schlenk filtered into a flask containing 338 mg (1.0 mmol) of K[Ph<sub>2</sub>B(pz)<sub>2</sub>] (pz = 1-C<sub>3</sub>H<sub>3</sub>N<sub>2</sub>) and 110 mg (1.0

mmol) of anhydrous  $[\text{Me}_4\text{N}]\text{Cl}$  in 150 mL of dry THF. The combined reaction mixture was stirred for an additional 3 h, during which time the solution gradually changed from green to orange. The solution was filtered through Celite to remove precipitated KCl, and the solvent was removed by rotary evaporation. The crude product was taken up in a minimum amount of absolute ethanol, the mixture was filtered through a fine glass frit, and the filtrate diluted with methylene chloride. Cooling this solution in a refrigerator resulted in the precipitation of pale red needles of  $[\text{Me}_4\text{N}][\mathbf{5}]$ , which were filtered and washed with diethyl ether (430 mg, 78%). Alternatively, reaction of 524 mg (1.0 mmol) of *closo*-3,3-( $\text{PhEt}_2\text{P}$ )<sub>2</sub>-3,1,2- $\text{NiC}_2\text{B}_9\text{H}_{11}$  with 338 mg of  $\text{K}[\text{Ph}_2\text{B}(\text{pz})_2]$  and 110 mg of  $[\text{Me}_4\text{N}]\text{Cl}$  in THF gave a comparable yield of product. Spectral data: <sup>1</sup>H NMR (acetone-*d*<sub>6</sub>, ambient temperature)  $\delta$  3.44 (s, NMe<sub>4</sub>), 3.74 (br s, carborane C-H), 6.06 (d, pz C-H), 7.00 (br, Ph C-H), 7.25 (t, pz C-H), 7.29 ppm (d, pz C-H); <sup>11</sup>B{<sup>1</sup>H} NMR  $\delta$  -22.5 (area 2), -20.3 (area 2), -13.7 (area 1), -12.2 (area 2), -3.2 (area 1), 1.82 ppm (area 1); characteristic IR (cm<sup>-1</sup>) 3055 (w), 3006 (w), 2599 (m, B-H str), 2527 (vs, B-H str), 2486 (s, B-H str), 1486 (m), 1432 (m), 1409 (m), 1291 (m), 1183 (s), 1144 (m), 1106 (m), 1067 (s), 746 (m), 722 (s), 709 (m); UV-vis  $\lambda_{\text{max}}$  302 nm. Anal. Calcd for C<sub>24</sub>H<sub>39</sub>B<sub>9</sub>N<sub>3</sub>Ni: C, 51.07; H, 6.97; B, 19.15; N, 12.41; Ni, 11.16. Found: C, 50.43; H, 7.02; B, 19.51; N, 12.32; Ni, 10.98.

**General Methods of Crystallographic Analyses.** All data were collected on an automated diffractometer in the  $\theta$ - $2\theta$  scan mode using Mo K $\alpha$  radiation. Data for **3a** and  $[\text{Me}_4\text{N}][\mathbf{5}]$  were collected on a modified Picker FACS-1 diffractometer. Data for **3b** were collected on a Huber diffractometer. All calculations were performed by using the DEC VAX 11/750 computer of the J. D. McCullough Crystallographic Laboratory and the UCLA crystallographic programs listed in the reference section.<sup>17</sup> Data were corrected for Lorentz and polarization effects. The structure of **3a** was solved by using direct methods (MULTAN80). Structures of **3b** and  $[\text{Me}_4\text{N}][\mathbf{5}]$  were solved by using heavy-atom methods. Remaining atoms were located by use of difference electron density maps. In the course of refinement all cage C and B atoms were initially assigned scattering factors for boron. After refinement, carboranyl carbon atom positions could be distinguished by their anomalously low temperature factors and by shorter interatomic distances. Reported *R* and *R<sub>w</sub>* values are defined as  $R = [\sum(|F_o| - |F_c|) / \sum|F_o|]$ ,  $R_w = [\sum w(|F_o| - |F_c|)^2 / \sum w|F_o|^2]^{1/2}$ , where  $w = 1/\sigma^2(F_o)$ , and "goodness of fit" is defined by  $[\sum w(|F_o| - |F_c|)^2 / (N_{\text{observns}} - N_{\text{variables}})]^{1/2}$ . Scattering factors for hydrogen were obtained from Stewart et al.,<sup>18</sup> and those for other atoms were taken from ref 19. Details of the individual data collections are given in Table IV.

**X-ray Analysis of 3a.** An orange crystal obtained by layering a chloroform solution of **3a** with absolute ethanol was attached to a fiber with epoxy cement. Systematic absences were found for reflections  $0k0$ ,  $k = 2n + 1$ . Unit cell parameters were determined from a least-squares fit of 30 accurately centered reflections ( $9.7^\circ < 2\theta < 20.0^\circ$ ). Three

intense reflections (10 $\bar{3}$ , 23 $\bar{2}$ , 200) were monitored every 97 reflections to check stability. Intensities of these reflections decayed only slightly, less than 5%, during the course of the experiment (29.9-h exposure). Anisotropic thermal parameters were refined for Rh and the C and N atoms of the pyrazole groups. All hydrogen atoms were kept in located positions with assigned *U* values of 0.0443 Å<sup>2</sup>. The dicarbollide cage exhibited a disorder such that only one atom could be assigned as C. The two adjacent atoms of the bonding face were treated as half C, and half B. This is a fairly common type of disorder for metallacarborane dicarbollide complexes.<sup>8</sup> Anomalous dispersion terms were applied to the scattering of Rh. A final difference electron density map was essentially featureless with the maximum and minimum peaks being ca. 1.1 e Å<sup>-3</sup> near two carbon atoms of the tris(1-pyrazolyl)borate ligand. Positional and thermal parameters for **3a** are given in the supplementary material.

**X-ray Analysis of 3b.** A red-orange crystal obtained by layering a methylene chloride solution of **3b** with *n*-pentane was affixed to a fiber with epoxy cement. Systematic absences were found for reflections  $hkl$ ,  $h + k = 2n + 1$ , and for  $h0l$ ,  $l = 2n + 1$ . Unit cell parameters were determined from a least-squares fit of 27 accurately centered reflections ( $10.0^\circ < 2\theta < 20.1^\circ$ ). Three intense reflections (3 $\bar{3}\bar{3}$ , 11 $\bar{5}$ , 15 $\bar{7}$ ) were monitored every 97 reflections to check stability. Intensities of these reflections did not decay during the course of the experiment (33.3-h exposure). Anisotropic thermal parameters were refined for Rh and carboranyl C and B atoms. All hydrogen atoms were kept in located positions with assigned *U* values of 0.08 Å<sup>2</sup>. Anomalous dispersion terms were applied to the scattering of Rh. A final difference electron density map was essentially featureless with the maximum and minimum peaks being ca. 0.7 e Å<sup>-3</sup>. Positional and thermal parameters for **3b** are given in the supplementary material.

**X-ray Analysis of [Me<sub>4</sub>N][5].** A brownish red needle obtained from THF/CH<sub>2</sub>Cl<sub>2</sub> was affixed to a fiber. Systematic absences were found for reflections  $0k0$ ,  $k = 2n + 1$ , and for  $h0l$ ,  $h = 2n + 1$ . Unit cell parameters were determined from a least-squares fit of 27 accurately centered reflections ( $7.6^\circ < 2\theta < 13.7^\circ$ ). Three intense reflections (20 $\bar{3}$ , 3 $\bar{1}\bar{1}$ , 021) were monitored every 97 reflections to check stability. Intensities of these reflections fluctuated only slightly, ca.  $\pm 5.5\%$ , with less than 3% decay during the course of the experiment (43.9-h exposure). Anisotropic thermal parameters were refined for N and Ni. The phenyl groups were kept rigid, C-C = 1.395 Å, C-H = 1.0 Å, and angles 120°. All carboranyl H and pyrazole atoms were kept in located positions. All other hydrogen atoms were kept in calculated positions with assigned *U* values of 0.10 (carboranyl, pyrazole), 0.10 (phenyl), and 0.12 (methyl) Å<sup>2</sup>. Anomalous dispersion terms were applied to the scattering of Ni. A final difference electron density map was essentially featureless with the maximum and minimum peaks being ca. 0.25 e Å<sup>-3</sup>. Positional and thermal parameters for  $[\text{Me}_4\text{N}][\mathbf{5}]$  are listed in the supplementary material. Unfortunately, only very small single crystals of this salt could be obtained (see Table IV). However, the precision of bond distances and angles is only marginally affected.

**Acknowledgment.** This work was funded by a grant from the National Science Foundation (CHE-88-06179). We thank Andrea Owyung for the illustrations.

**Supplementary Material Available:** Tables of atomic coordinates, thermal parameters, and bond lengths and angles for **3a**, for **3b/3b'**, and for **5** (22 pages); tables of final observed and calculated structure factors for **3a**, for **3b/3b'**, and for **5** (41 pages). Ordering information is given on any current masthead page.

- (17) Programs: CARESS (Broach, Coppens, Becker, Blessing), peak profile analysis, Lorentz and polarization corrections; ORFLS (Busing, Martin, Levy), structure factor calculation, full-matrix least-squares refinement; MULTAN80 (Main, Fiske, Hull, Lessinger, Germain, Declercq, Woolfson); ORTEP (Johnson), figure plotting.  
 (18) Stewart, R. F.; Davidson, E. R.; Simpson, W. T. *J. Chem. Phys.* **1965**, *42*, 3175.  
 (19) *International Tables for X-ray Crystallography*; Kynoch: Birmingham, England, 1974; Vol. IV.